



ZIBELINE INTERNATIONAL™
PUBLISHING
ISSN: 2773-6202 (Online)
CODEN: JTIOCC



RESEARCH ARTICLE

MODEL BASED ROBOT CALIBRATION TECHNIQUE WITH CONSIDERATION OF JOINT COMPLIANCE

Hoai-Nhan Nguyen*, Trong-Hai Nguyen, Dinh-Tung Vo, Quoc-Phuong Pham

HUTECH Institute of Engineering, Ho Chi Minh City University of Technology (HUTECH), Ho Chi Minh City, Vietnam

*Corresponding Author Email: nh.nhan@hutech.edu.vn

This is an open access article distributed under the Creative Commons Attribution License CC BY 4.0, which permits unrestricted use, distribution, and reproduction in any medium, provided the original work is properly cited.

ARTICLE DETAILS

Article History:

Received 15 January 2021
Accepted 19 February 2021
Available online 2 March 2021

ABSTRACT

Robot accuracy plays an important role for robot based application in advanced industry. Especially, robot accuracy decreases because of structural deformation when robot carries heavy load. Identification of physical robot parameters improves its accuracy by updating robot model parameters which are used in robot controller. This research presents identification technique of robot geometric parameters and its joint deformation joint angle. The target of the paper is comparison of two cases 1) only geometric calibration and 2) geometric and joint deformation angles calibration. Simulation calibration is performed on a Hyundai 800 robot which is designed for carrying heavy loads. The robot position accuracy after calibration demonstrates the effectiveness and correctness of the method.

KEYWORDS

Kinematic identification, Joint stiffness, robot calibration.

1. INTRODUCTION

Movement programming of robot can be performed on-site or off-site. On-site programming shows weak points of only using in cases of a small number of robots. While off-site programming can transfer controlling program for a big number of robots at a time. However, actual robot parameters normally differ from the robot model parameters which are installed in robot controller (supplied by robot manufacturer). This difference leads a physical robot come to a wrong targets. So, it is necessary to update robot parameters by robot calibration process.

Previous studies concentrated on modeling robot geometric error sources for purposes of calibration (Whitney et al., 1986; Schröder et al., 1997; Alici and Shirinzadeh, 2005). These errors are composed of two types: geometric and non-geometric errors. Geometric errors are link twist angle, link length errors, link and joint angle offsets. Non-geometric errors can be listed as gear backlash, joint deflection, link compliance, etc. Some researchers assumed that only geometric errors exist on robots kinematic model (Benjamin et al., 1991; Hayati et al., 1988; Veitschegger and Wu, 1986; Khalil et al., 1990; Park et al., 2011). Other researchers (To and Webb, 2012; Gong et al., 2000) considered both link geometric and non-geometric errors (only joint deflection) robot models. The deformation of robot joints and links are caused by its weights and carried payloads; and it really affects robot position Duellen and Schroer, 1991; Hudgens et al., 1991). To solve the problem of existence of robot physical deformation, Dullen et al. applied a theory of flexible beams to study the effects of link compliance. The research of Hudgen et al. identified general robot deflection characteristics by applied torques and forces. Both works should include other non-geometric errors to obtain more accurate robot

model. Acilli et al. utilized Fourier polynomial for predicting the position error caused by the non-geometric error (Alici and Shirinzadeh, 2005). By applying the method, a huge number of training data need to be collected, non-linear relationship of joint input and position output is not guarantee for all robot poses. Artificial Neural Network (ANN) has more advantageous characters: learning ability, adaptation, and flexibility. Some studies have using the ANN to compensate for robot position errors (Joon et al., 2001; Aoyagi et al., 2010; Wang et al., 2012; Takanashi, 1990; Zhong et al., 1996). Jang et al. used a Radial Basis Function Network (RBFN) to form a relation input is joint positions and output is joint offset. The works have utilized an ANN to make the relationship of end-effector positions and corresponding position errors. However, each robot configurations produce different error even the same end-point position (Meggiolaro et al., ; Zhong and Lewis, 1995). However, application of ANN for robot error compensation still has some drawback because unknowing the robot error sources, difficult to embed the algorithm into the robot controller.

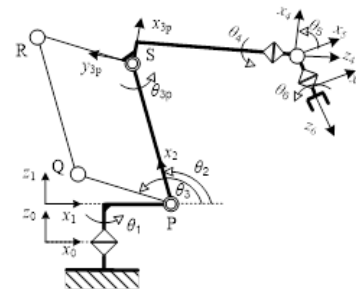


Figure 1: A schematic of the HH800 robot and attached link frames

Quick Response Code



Access this article online

Website:
<https://jtin.com.my/>

DOI:
10.26480/jtin.01.2021.06.09

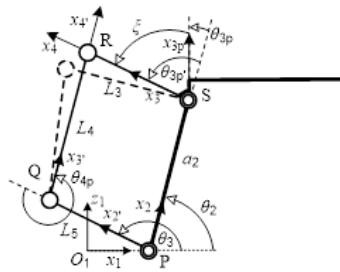
In this paper, we present a technique for the calibration of industrial robots by considering both source of errors such as geometric and non-geometric error to obtain the robot model so closes to the physical robot. The proposed method models the robot joint compliance errors as a rotational spring. Because of small deflection of robot joint shaft, functional stiffness relationship is assumed linear. Simulation calibration for the Hyundai HH800 robot was carried out to demonstrate the effectiveness and correctness of the proposed method. The simulation results show the more accuracy if we include joint deflection value to robot model.

2. KINEMATIC MODEL OF THE HH800 ROBOT

2.1 Kinematic model of HH800 robot

HH800 robot (Fig. 1) has 6 degree of freedom (dof), consists of a main open kinematic chain (6 dof) and a closed loop mechanism (2 dof). The open chain is form by the revolute joints 1, 2, 3p, 4, 5, and 6 and corresponding links. The closed mechanism PQRS is connected by the joints 2, 3, Q, R and S. The frames are attached at links by using Danevit-Hartenberg (D-H) convention (Hartenberg et al., 1955). Table 1 shows nominal D-H parameters of the robot. A transformation matrix of two link frames $\{i-1\}$ and $\{i\}$ is formed by:

$${}^{i-1}T = Rot(x_{i-1}, \alpha_{i-1}) \cdot Tr(x_{i-1}, a_{i-1}) \cdot Tr(z_i, d_i) \cdot Rot(z_i, \theta_i) \quad (1)$$



where, twist angle α_{i-1} , link length a_{i-1} , link offset d_i , and joint variable θ_i ; $Rot(\cdot)$ and $Tr(\cdot)$ are rotation and translation matrice (Craig, 1989).

A transformation from the robot base frame to the end-effector frame is composited by:

$${}^0T = {}^0T(\theta_1) \cdot {}^1T(\theta_2) \cdot {}^2T(\theta_{3p}) \cdot {}^3T(\theta_4) \cdot {}^4T(\theta_5) \cdot {}^5T(\theta_6) \cdot {}^6T \quad (2)$$

where ${}^{i-1}T$ is computed by (1), $i = 2, \dots, 6$. The matrix 0T is computed by

$${}^0T = Tr(x_0, a_0) \cdot Tr(y_0, b_0) \cdot Tr(z_1, d_1) \cdot Rot(x_0, \alpha_0) \cdot Rot(y_0, \beta_0) \cdot Rot(z_1, \theta_1) \quad (3)$$

the matrix 6T is computed by:

$${}^6T = Tr(x_6, a_6) \cdot Tr(y_6, b_6) \cdot Tr(z_7, d_7) \quad (4)$$

and the matrix ${}^2T(\theta_{3p})$ in (2) is computed with the passive joint angle θ_{3p} . The angle θ_{3p} is solved through a constraint equations of the closed mechanism PQRS (Fig. 2) with input value of joint angles θ_2 and θ_3 . For simplicity, it does not lose the generality, mechanism PQRS is treated as a planar mechanism. The output and input angles relates as following equation express in the plane $O_1x_1z_1$ as follows:

$$\begin{aligned} a_2 c \theta_2 + L_3 c \theta_{2,3p} - L_5 c \theta_3 - L_4 c \theta_{3,4p} &= 0 \\ a_2 s \theta_2 + L_3 s \theta_{2,3p} - L_5 s \theta_3 - L_4 s \theta_{3,4p} &= 0 \end{aligned} \quad (5)$$

where $c\theta_i$ and $s\theta_i$ are short forms of $\cos(\theta_i)$ and $\sin(\theta_i)$, respectively, and $\theta_{h,k} = \theta_h + \theta_k$, $L_5 = PQ$, $L_4 = QR$, $L_3 = RS$, $a_2 = SP$.

The closed loop PQRS is a parallelogram, then $L_4 = a_2$ and $L_5 = L_3$ (Figs.1 and 2). The output joint position θ_{3p} can be found by (5) with input joint values θ_2 and θ_3 : $\theta_{3p} = \theta_{3p} - \xi$, where $\theta_{3p} = \theta_3 - \theta_2$ and $\xi = 90^\circ$ is a constant angle. This transformation matrix 2T should be modified as in the researc to adapt to the properties of the calibration robot model: complete, proportional, and continuous. Matrix 2T is modified as follows:

$${}^2T = Rot(x_2, \alpha_2) \cdot Tr(x_2, a_2) \cdot Rot(y_2, \beta_2) \cdot Rot(z_{3p}, \theta_{3p}) \quad (6)$$

where β_2 is the link twist angle about the axis y_2 .

2.2 Robot joint compliance model

In a robot static pose, a robot joint torque causes a rotational deformation about a joint shaft. Then a joint shaft is considered as a torsional spring. In this section, we propose a torsional spring model to represent rotational joint compliance. The relation of input moment M and deformation angle $\delta\theta$ of torsional springs, for instance $M = k(\delta\theta)^3$. For small $\delta\theta$, the relation can be assumed linear as follows:

$$\delta\theta_i = \frac{1}{k_i} M_i = s_i M_i \quad (7)$$

where M_i [Nm]: joint torque at joint axis i , k_i [Nm/rad] stiffness coefficient of joint i , s_i [rad/Nm] compliance coefficient, $\delta\theta_i$ [°] is the deformation angle of joint i , $i = 1, \dots, 6$.

Table 1: D-H parameters of HH800 robot (units: length [m], angle [°]; “-” unavailable)

DH parameters of the main open chain						
i	α_{i-1}	a_{i-1}	β_{i-1}	b_{i-1}	d_i	θ_i
1	0	0	0	0	1.2	θ_1
2	90	0.515	-	-	0	θ_2
3	0	1.6	0	-	0	θ_3
4	90	0.35	-	-	1.9	θ_4
5	-90	0	-	-	0	θ_5
6	90	0	-	-	0.445	θ_6
Tool	-	0.2	-	0.2	0.2	-
Link lengths of the closed loop						
L_5	0.8	L_4	1.6	L_3	0.8	

The active joint torques are computed by the methods presented in the studies (Luh et al., 1985; Nakamura et al., 1989). By applying a virtual work principle and an open tree-structure (joint R of the closed loop PQRS (Figs.1 and 2) is cut open). The first chain is connected by the joints θ_1 , θ_2 , θ_{3p} , θ_4 , θ_5 , and θ_6 . The second is connected by the joints θ_1 , θ_3 , Q, and R. As a result, the active robot joint torques are M_1, M_2, M_3, M_4, M_5 , and M_6 . Static joint torques calculation requires data of the robot dynamic parameters, such as link weights, link mass centers' positions, and payload.

3. FORMULATION FOR PARAMETER IDENTIFICATION

Differential transformation of the open kinematic chain can be obtained by differentiating equations (2) in term of its kinematic parameters as follows:

$$\Delta X = J \cdot \Delta P \quad (8)$$

where ΔX is (3×1) vector of 3 position errors of the robot tip. $\Delta P = [\Delta\alpha \Delta a \Delta\beta \Delta b \Delta d \Delta\theta]^T$ is a $(p \times 1)$ vector of kinematic errors. $\Delta\alpha$ is a $(N_\alpha \times 1)$ vector of link twist errors $\Delta\alpha_i$, Δa is a $(N_a \times 1)$ link length errors Δa_i , $\Delta\beta$ is a $(N_\beta \times 1)$ link twist errors $\Delta\beta_i$, Δb is a $(N_b \times 1)$ link length errors Δb_i , Δd is a $(N_d \times 1)$ link offset errors Δd_i , and $\Delta\theta$ is a $(N_\theta \times 1)$ joint offsets $\Delta\theta_i$. $J_\alpha = [J_{\alpha_i}]$, $J_a = [J_{a_i}]$, $J_\beta = [J_{\beta_i}]$, $J_b = [J_{b_i}]$, $J_d = [J_{d_i}]$, and $J_\theta = [J_{\theta_i}]$ are the sub-matrices whose columns are computed by following the published work [25]. The position constraints (5) can be expressed in the following form:

$$\theta_{3p} = f(\theta_2, \theta_3, L_5, L_4), \quad (10)$$

By the expansion of (8):

$$\Delta X = J_{\alpha_0} \Delta\alpha_0 + \dots + J_{a_2} \Delta a_2 + \dots + J_{\theta_2} \Delta\theta_2 + J_{\theta_{3p}} \Delta\theta_{3p} + J_{\theta_4} \Delta\theta_4 + \dots, \quad (11)$$

Robot consists of a main open chain and a closed loop mechanism (Fig.1), robot identification equations are formed by including the differential output variable the closed loop θ_{3p} into differential transformation of the open kinematic chain at according variable θ_{3p} . By differentiating the variable θ_{3p} in terms of the parameters $\theta_2, \theta_3, L_5, L_4$, to obtain:

$$\Delta\theta_{3p} = \frac{\partial f}{\partial \theta_2} \Delta\theta_2 + \frac{\partial f}{\partial \theta_3} \Delta\theta_3 + \frac{\partial f}{\partial L_5} \Delta L_5 + \frac{\partial f}{\partial L_4} \Delta L_4, \quad (12)$$

Substituting (12) into (11), we have the following equation at θ_{3p} :

$$\begin{aligned} \Delta X = J_{\alpha_0} \Delta\alpha_0 + \dots + J_{a_2} \Delta a_2 + \dots + J'_{\theta_2} \Delta\theta_2 + J'_{\theta_3} \Delta\theta_3 + J_{\theta_4} \Delta\theta_4 + \dots \\ + J'_{L_5} \Delta L_5 + J'_{L_4} \Delta L_4 = J' \cdot \Delta P', \end{aligned} \quad (13)$$

where column vectors J'_{θ_2} and J'_{θ_3} for joint angles θ_2 and θ_3 , column vectors J'_{L_5} and J'_{L_4} for parameters L_5 and L_4 , respectively:

$$J'_{\theta_2} = J_{\theta_{3p}} \frac{\partial f}{\partial \theta_2} + J_{\theta_2} J'_{\theta_3} = J_{\theta_{3p}} \frac{\partial f}{\partial \theta_3}, J'_{L_5} = J_{\theta_{3p}} \frac{\partial f}{\partial L_5}, J'_{L_4} = J_{\theta_{3p}} \frac{\partial f}{\partial L_4}, \quad (14)$$

Equation (13) describes the relationship between robot geometric errors and its robot tool tip errors. The effects of joint compliance is included to (13) by being modified as follows:

$$\Delta X = J' \cdot \Delta P' + J'_{\theta} \cdot \delta \theta \quad (15)$$

where matrix $J'_{\theta} = [J'_{\theta_i}]$ is computed by (9) ($i = 1, \dots, 6$), $\delta \theta = [\delta \theta_i]^T$ is a vector of joint compliance:

$$[\delta \theta_i] = \text{diag}[M_i] \cdot [s_i]^T = M \cdot s \quad (16)$$

$M = \text{diag}[M_i]$, M_i is the i^{th} joint torque; $s = [s_i]^T$ is the vector of joint compliance s_i , $i = 1, \dots, 6$. Substituting (16) into (15) to obtain the identification equation of the robot kinematic errors:

$$\Delta X = [J' \quad J'_{\theta} \cdot \text{diag}[M_i]] \begin{bmatrix} \Delta P' \\ s \end{bmatrix} \quad (17)$$

$$H = [J' \quad J'_{\theta} \cdot \text{diag}[M_i]], \Delta X = X_m - X, \quad (18)$$

The solution of equation (17) in the sense of least squares:

$$\begin{bmatrix} \Delta P' \\ s \end{bmatrix} = (H^T H)^{-1} H^T \Delta X; \quad \Delta X = \delta X_g + \delta X_c \quad (19)$$

where X_m is a (3×1) vector of the measured end-effector position, δX_g is the robot position error due to link geometric errors, δX_c is the robot position error due to joint angle deformation.

5. SIMULATION AND RESULTS

Table 2: Absolute position accuracy of the HH800 robot (calibration)

	Mean[mm]	Max.[mm]
Before calibration (nominal robot model)	29,74	46.82
Calibration with robot link geometry	0.453	1.40
Calibration with robot link geometry and joint compliance	0.1	0.28

A robot calibration system consists of a Hyundai HH800 robot; an assumed 3D point measurement device (measurement accuracy of 0.01 mm/m, repeatability of +/-0.006 mm/m). Measurement position is defined at a point E on robot tool. The three-dimensional coordinates of the end points are measured by the assumed measuring device and saved in a computer; the associated robot joint readings also are recorded. In the identification process, we identify the robot link geometric errors and joint compliance parameters by using the above measurement. The total number of identifiable parameters is 29 (25 geometric and 4 joint compliance parameters, s_2, s_3, s_4, s_5). Because the first joint axis is vertical, the s_1 torsional deformation about the first axis is so small compared with other joint, s_1 deformation does not effects much and can be neglected.

The simulation results show that (Table 2) before calibration the mean end-point deviation of robot is 29,74 [mm], this number decrease to 0.453 mm for case geometric parameter calibration, the number is reduced to 0.1 mm for case geometric and stiffness parameter calibration. The stiffness parameters of joints 2, 3, 4, 5 are $s_2 = 1.792 \times 10^7$ [rad/Nm], $s_3 = 1.915 \times 10^7$ [rad/Nm], $s_4 = 1.959 \times 10^7$ [rad/Nm], and $s_5 = 1.820 \times 10^7$ [rad/Nm], respectively. Maximum values of robot end-point deviation are shown in the third column of Table 2 accordingly.

6. CONCLUSIONS

This paper suggested a model based calibration method for increasing robot position accuracy. The method has many advantages such as less computing time, fast convergence, and accurate knowledge of error sources. The simulation was performed on the Hyundai HH800 robot show that robot average accuracy is increased significantly to 0.1 [mm] (from 29, 74 [mm] before calibration). The simulation calibration results show that the including joint deformation into robot model for case of robot carrying load is necessary.

REFERENCES

- Alici G, and Shirinzadeh B. 2005. A systematic technique to estimate positioning errors for robot accuracy improvement using laser interferometry-based sensing. *Mechanism and Machine Theory*; 40: 879-906.
- Aoyagi S., and et al. 2010. Improvement of robot accuracy by calibrating kinematic model using a laser tracking system-compensation of non-geometric errors using neural networks and selection of optimal measuring points using genetic algorithm. In: *IEEE Int. Conf. on Intelligent Robotics and Systems (IROS)*, Taipei, Taiwan, 18-22 Oct, pp.5660-5665
- Benjamin W. M., Zvi S. R., Morris R. D. 1991. *Fundamental of Manipulator calibration*. Inc. New York: John Wiley & Son.
- Bennett D.J. and Hollerbach J.M. 1991. Autonomous Calibration of Single-Loop Closed Kinematic Chains Formed by Manipulators with Passive End point Constraints. *IEEE Trans. on Robotics and Automation*; 7:597-606.
- Craig J.J. 1989. *Introduction to Robotics: Mechanics and control*. Second ed. Addison-Wiley, pp. 83-100.
- Duelen G. and Schroer K. 1991. *Robot Calibration Method and Results*, Robotics and Computer Integrated Manufacturing; 8: 223-231.
- Gong C., Yuan J., and Ni J. 2000. Non-geometric error identification and compensation for robotic system by inverse calibration. *J. of Machine Tools and Manufacture*; 40:2119-2137.
- Hartenberg R.S. and Denavit J. 1955. A kinematic notation for lower pair mechanisms based on matrices. *Trans. ASME/ Jour. of App. Mech*; 77:215-221.
- Hayati S., Tso K., Roston G. 1988. Robot Geometry Calibration. In: *Proc. IEEE Int. Conf. on Robotics and Automation*, 2, pp. 947-951.
- Hudgens J. C., Hernandez E., and Tesar D. 1991. *A compliance parameter estimation method for serial manipulator DSC*. Applications of Modeling and Identification to Improve Machine Performance ASME; 29:15-23.
- Joon H.J., Soo H.K., and Yoon K.K. 2001. Calibration of geometric and non-geometric errors of an industrial robot. *Robotica*. 19: 311-321 DOI :10.1017/S0263574700002976
- Khalil W., Caenen J. L. and Enguehard Ch. 1990. Identification and Calibration of the Geometric Parameters of Robots. *The First Int. Symposium on Experimental Robotics I*, pp. 528-538
- Luh J.Y.S. and Zheng Y.F. 1985. Computation of input generalized forces for robots with closed kinematic chain mechanisms. *IEEE J. of Robotics and Automation*; 1: 95-103.
- Meggiolaro M.A., Scriffignano G., and Dubowsky S. 2000. Manipulator Calibration Using a Single End Point Contact Constraint. *Proc. of DETC, ASME*, Sep. 10-14, DETC2000/MECH-14129, Baltimore, MD.
- Nakamura Y, and Ghodoussi M. 1989. Dynamics computation of closed-link robot mechanisms with non-redundant and redundant actuators. *IEEE Transactions on Robotics and Automation*; 5:294-302.
- Park I.W., et al. 2011. Laser-Based Kinematic Calibration of Robot Manipulator Using Differential Kinematics, *IEEE/ASME Trans. on Mechatronics*; 99:1-9.
- Schröer K., and et al. 1997. Complete, Minimal and Model-Continuous Kinematic Models for Robot Calibration. *Robotics and Computer-Integrated Manufacturing*; 13: 73-85.
- Siciliano B., Sciavicco L., and Villani L. 2009. *Robotics Modeling, Planning and Control*. Springer, BERLIN, pp. 70-72.

Takanashi N. 1990. 6 DOF Manipulators Absolute Positioning Accuracy Improvement Using a Neural-Network. Proc. IEEE Int. Workshop on Intel. Robots and Systems; 2:635-640.

To M. and Webb P. 2012. An improved kinematic model for calibration of serial robots having closed-chain mechanisms. *Robotica*; 30: 963-971 DOI:10.1017/S0263574711001184

Veitschegger W., Wu C. 1986. Robot Accuracy Analysis Based on Kinematics, *IEEE J. of Robotics and Automation*; 2:171-179.

Wang D., Bai Y., and Zhao J. 2012. Robot manipulator calibration using neural network and a camera-based measurement system. *Transactions of the Institute of Measurement and Control*; 34:105-121.

Whitney D.E., Lozinski C.A. and Rourke J.M. 1986. Industrial Robot Forward Calibration Method and Results, *J. Dynamic Systems, Measurement and Control*; 108:1-8.

Zhong X., Lewis J., and Nagy F.L.N. 1996. Inverse robot calibration using artificial neural networks. *Engineering Applications of Artificial Intelligence* Feb; 9: 83-93.

Zhong X.L. and Lewis J.M. 1995. A New Method for Autonomous Robot Calibration. In: *Int. Conf. on Robotics and Automation*; 2:1790-1795.

Zvi S. R., Benjamin W. M. and Bahram R. 1987. An overview of robot calibration. *IEEE Journal of Robotics and Automation*; 3:377-385.

